Treating the Gibbs phenomenon in barycentric rational interpolation and approximation via the S-Gibbs algorithm

J.-P. Berrut [a], S. De Marchi [b], G. Elefante [a], F. Marchetti [c,*]

[a] *Département de Mathématiques, Université de Fribourg, Switzerland*
[b] *Dipartimento di Matematica "Tullio Levi-Civita", Università di Padova, Italy*
[c] *Dipartimento di Salute della Donna e del Bambino, Università di Padova, Italy*

A B S T R A C T

In this work, we extend the so-called mapped bases or *fake nodes* approach to the barycentric rational interpolation of Floater–Hormann and to AAA approximants. More precisely, we focus on the reconstruction of discontinuous functions by the *S-Gibbs* algorithm introduced in De Marchi et al. (2020). Numerical tests show that it yields an accurate approximation of discontinuous functions.

Keywords:
Barycentric rational interpolation
Gibbs phenomenon
Floater–Hormann interpolant
AAA algorithm
Fake nodes

1. Introduction

In the seminal paper [1], Floater and Hormann (FH) have introduced a family of linear barycentric rational interpolants, which contains the first Berrut interpolant [2,3]. FH interpolants have shown good approximation properties for smooth functions, in particular using equidistant nodes. Because of their high accuracy, these interpolants have been applied in several frameworks, such as for solving Volterra integral equations [4], or as collocation methods for nonlinear parabolic partial differential equations [5]. Among other favorable properties, the Lebesgue constant grows logarithmically with the number of nodes [6]. Other instances in which linear barycentric rational interpolation is extremely efficient, actually exponentially convergent, are the trigonometric interpolant presented in [2] and used with conformally mapped equispaced points [7,8], and its special case on the interval, Berrut's second interpolant [3] between conformally mapped Chebyshev points [9]. The Berrut interpolants enjoy a Lebesgue constant that grows logarithmically for a wide class of nodes as well [10,11].

* Corresponding author.
E-mail addresses: jean-paul.berrut@unifr.ch (J.-P. Berrut), demarchi@math.unipd.it (S. De Marchi), giacomo.elefante@unifr.ch (G. Elefante), francesco.marchetti.1@phd.unipd.it (F. Marchetti).

In [12], the *Adaptive Antoulas-Anderson* (AAA) greedy algorithm for computing a barycentric rational approximant has been presented. This recent method leads to impressively well-conditioned bases, which can be used in various fields, such as in computing conformal maps, or in rational minimax approximations (see [13,14]). Note that a similar approach has been considered in [15] for kernel-based interpolation.

The FH interpolants and the approximants obtained by the AAA algorithm suffer from the well-known *Gibbs phenomenon*, when the underlying function presents jump discontinuities. For a general overview of that phenomenon, interested readers may refer to [16,17].

In [18], a new interpolation procedure has been suggested in the framework of univariate polynomial interpolation to reduce the Gibbs phenomenon. The method essentially maps the polynomial basis, in which the interpolant is expressed, by a suitable map S, or equivalently uses the so-called *fake nodes*, without resampling the underlying function. This led to the *S-Gibbs* algorithm, which basically constructs the map S that is then used for eliminating the Gibbs effect (see *S-Gibbs* [18, Algorithm 2]).

In this work, we propose an extension of the fake nodes approach (cf. [18]) to the framework of barycentric rational interpolation, focusing on FH interpolants and the AAA algorithm.

2. Barycentric polynomial interpolation

Let $\mathcal{X}_n := \{x_i : i = 0, \dots, n\}$ be a set of $n+1$ distinct nodes in $I = [a, b] \subset \mathbb{R}$, increasingly ordered from $x_0 = a$ to $x_n = b$. We consider the problem of interpolating a function $f : I \longrightarrow \mathbb{R}$ given the set of samples $\mathcal{F}_n := \{f_i = f(x_i) : i = 0, \dots, n\}$.

It is well-known (see e.g. [19]) that it is possible to write the unique interpolating polynomial $P_n[f]$ of degree at most n of f at $\mathcal{X}_n$ for any $x \in I$ in the second barycentric form

$$P_n[f](x) = \frac{\sum_{i=0}^{n} \frac{\lambda_i}{x-x_i} f_i}{\sum_{i=0}^{n} \frac{\lambda_i}{x-x_i}} , \tag{1}$$

where $\lambda_i = \prod_{j \neq i} \frac{1}{x_i - x_j}$ are the so-called *weights*. This expression is one of the most stable formulas for evaluating $P_n[f]$ (see [20]). If the weights λ_i are changed to other nonzero weights, say w_i, then the corresponding barycentric rational function

$$r_n[f](x) = \frac{\sum_{i=0}^{n} \frac{w_i}{x-x_i} f_i}{\sum_{i=0}^{n} \frac{w_i}{x-x_i}} \tag{2}$$

still satisfies the interpolation conditions $r_n[f](x_i) = f_i, \; i = 0, \dots, n$. For more details about barycentric rational interpolation, we refer to [19].

2.1. The Floater–Hormann family

Let $n \in \mathbb{N}$, $d \in \{0, \dots, n\}$. Let p_i, $i = 0, \dots, n-d$ denote the unique polynomial interpolant of degree at most d interpolating the $d+1$ points $(x_k, f_k), \; k = i, \dots, i+d$. One can write the FH rational interpolant as

$$R_{n,d}[f](x) = \frac{\sum_{i=0}^{n-d} \lambda_i(x) p_i(x)}{\sum_{i=0}^{n-d} \lambda_i(x)}, \text{ where } \lambda_i(x) = \frac{(-1)^i}{(x-x_i)\cdots(x-x_{i+d})},$$

which interpolates f at the set of nodes $\mathcal{X}_n$. It has been proved in [1] that $R_{n,d}[f]$ has no real poles and that it reduces to the unique interpolating polynomial of degree at most n when $d = n$.

One can derive the barycentric form of this family of interpolants as well. Indeed, with considering the sets $J_i = \{k \in \{0, 1, \dots, n-d\} : i - d \leq k \leq i\}$, one has

$$R_{n,d}[f](x) = \frac{\sum_{i=0}^{n} \frac{w_i}{x-x_i} f_i}{\sum_{i=0}^{n} \frac{w_i}{x-x_i}}, \text{ where } w_i = (-1)^{i-d} \sum_{k \in J_i} \prod_{\substack{j=k \\ j \neq i}}^{j+d} \frac{1}{|x_i - x_j|}.$$

2.2. The AAA algorithm

Let us consider a set of points $\mathcal{X}_N$ with a large value of N and a function f. The *AAA algorithm* [12] is a greedy technique that in the step $m \geq 0$ considers the set $\mathcal{X}^{(m)} = \mathcal{X}_N \setminus \{x_0, \dots, x_m\}$ and constructs the interpolant

$$r_m[f](x) = \frac{\sum_{i=0}^{m} \frac{w_i}{x-x_i} f_i}{\sum_{j=0}^{m} \frac{w_j}{x-x_j}} = \frac{n(x)}{d(x)},$$

by solving the discrete least squares problem

$$\min \|fd - n\|_{\mathcal{X}^{(m)}} \qquad \|\boldsymbol{w}\|_2 = 1,$$

for the unknown vector $\boldsymbol{w} = (w_0, \dots, w_m)$, where $\|\cdot\|_{\mathcal{X}^{(m)}}$ is the discrete 2-norm over $\mathcal{X}^{(m)}$. The subsequent data site $x_{m+1} \in \mathcal{X}^{(m)}$ is chosen by maximizing the residual $|f(x) - n(x)/d(x)|$ with respect to $x \in \mathcal{X}^{(m)}$.

3. Mapped bases and fake nodes in barycentric rational interpolation

Here we investigate the extension of the interpolation method presented in [18] to the *Floater–Hormann* interpolants and to the approximants produced via the *AAA algorithm*.

Let $S : I \longrightarrow \mathbb{R}$ be a mapping that we assume injective. We construct the "new" interpolant $r_n^S : I \longrightarrow \mathbb{R}$ at the nodes $\mathcal{X}_n$ and function values $\mathcal{F}_n$ as

$$r_n^S[f](x) := \frac{\sum_{i=0}^{n} \frac{w_i}{S(x)-S(x_i)} f_i}{\sum_{i=0}^{n} \frac{w_i}{S(x)-S(x_i)}}.$$

As discussed in [18, p. 3] in the polynomial interpolation setting, we can see $r_n^S[f]$ from two different perspectives.

First, since the interpolant $r_n[f]$ defined in (2) admits a cardinal basis form $r_n[f](x) = \sum_{j=0}^{n} f_j b_j(x)$, where $b_j(x) = \frac{\frac{w_j}{x-x_j}}{\sum_{i=0}^{n} \frac{w_i}{x-x_i}}$ is the jth basis function, in the same spirit, we can write $r_n^S[f]$ in the mapped cardinal basis form $r_n^S[f](x) = \sum_{i=0}^{n} f_i b_i^S(x)$, where $b_j^S(x) = \frac{\frac{w_j}{S(x)-S(x_j)}}{\sum_{i=0}^{n} \frac{w_i}{S(x)-S(x_i)}}$ is the jth mapped basis function.

Using the S mapping approach, a more stable interpolant may arise. We present an upper bound on the S-Lebesgue constant which involves the classical Lebesgue constant.

Theorem 1. *Let $\Lambda_n(\mathcal{X}_n) = \max_{x\in I} \sum_{j=0}^{n} |b_j(x)|$ and $\Lambda_n^S(\mathcal{X}_n) := \max_{x\in I} \sum_{j=0}^{n} |b_j^S(x)|$ be the classical and the S-Lebesgue constants, respectively. We then have*

$$\Lambda_n^S(\mathcal{X}_n) \leq C \Lambda_n(\mathcal{X}_n),$$

where $C = \frac{\max_k A^k}{\min_k A_k}$ with

$$A^k = \max_{x\in I} \prod_{\substack{l=0 \\ l\neq k}}^{n} \left| \frac{S(x) - S(x_l)}{x - x_l} \right|, \quad A_k = \min_{x\in I} \prod_{\substack{l=0 \\ l\neq k}}^{n} \left| \frac{S(x) - S(x_l)}{x - x_l} \right|.$$

Proof. We bound each basis function b_j^S in terms of b_j for all $x \in I$. We compute

$$
\begin{aligned}
|b_j^S(x)| &= \left| \frac{\frac{w_j}{S(x)-S(x_j)}}{\sum_{i=0}^n \frac{w_i}{S(x)-S(x_i)}} \right| = \left| \frac{\frac{w_j}{S(x)-S(x_j)} \prod_{l=0}^n (S(x)-S(x_l))}{\sum_{i=0}^n \frac{w_i}{S(x)-S(x_i)} \prod_{l=0}^n (S(x)-S(x_l))} \right| \\
&= \left| \frac{w_j \prod_{\substack{l=0 \\ l\neq j}}^n (S(x)-S(x_l))}{\sum_{i=0}^n w_i \prod_{\substack{l=0 \\ l\neq i}}^n (S(x)-S(x_l))} \right| \\
&= \left| \frac{w_j \prod_{\substack{l=0 \\ l\neq j}}^n (S(x)-S(x_l)) \left(\frac{\prod_{\substack{m=0 \\ m\neq j}}^n x-x_m}{\prod_{\substack{m=0 \\ m\neq j}}^n x-x_m} \right)}{\sum_{i=0}^n w_i \prod_{\substack{l=0 \\ l\neq i}}^n (S(x)-S(x_l)) \left(\frac{\prod_{\substack{m=0 \\ m\neq i}}^n x-x_m}{\prod_{\substack{m=0 \\ m\neq i}}^n x-x_m} \right)} \right| \\
&= \left| \frac{\frac{w_j}{x-x_j} \prod_{\substack{l=0 \\ l\neq j}}^n \frac{S(x)-S(x_l)}{x-x_l}}{\sum_{i=0}^n \frac{w_i}{x-x_i} \prod_{\substack{l=0 \\ l\neq i}}^n \frac{S(x)-S(x_l)}{x-x_l}} \right| \\
&\leq \frac{\max_k A^k}{\min_k A_k} \left| \frac{\frac{w_j}{x-x_j}}{\sum_{i=0}^n \frac{w_i}{x-x_i}} \right| = \frac{\max_k A^k}{\min_k A_k} |b_j(x)| = C|b_j(x)|. \quad \square
\end{aligned}
$$

Second, equivalently to the above mapped basis perspective, we can discuss the construction of the interpolant $r_n^S[f]$ via the so-called fake nodes approach. Let $\tilde{r}_n[g]$ be the barycentric interpolant as in (2) that interpolates, at the set of fake nodes $S(\mathcal{X}_n)$, the function $g : S(I) \longrightarrow \mathbb{R}$, making use of the same functional values $\mathcal{F}_n$, that is

$$
g_{|_{S(\mathcal{X}_n)}} = f_{|_{\mathcal{X}_n}}.
$$

Observe that $r_n^S[f](x) = \tilde{r}_n[g](S(x))$ for every $x \in I$. Hence, we may also build $r_n^S[f]$ upon a standard barycentric interpolation process, thereby providing a more intuitive interpretation of the method.

The choice of the mapping S is crucial for the accuracy of the proposed interpolant $r_n^S[f]$. Here, we assume that f presents jump discontinuities and we adopt the so-called *S-Gibbs* Algorithm (SGA) [18] to construct an effective mapping S.

4. Numerical examples

In this section, we test the fake nodes approach with SGA in the framework of FH interpolants and the AAA algorithm for approximation. We fix $k = 10$ in the SGA. As observed in [18], also in this setting the choice of the shifting parameter is non-critical as long as it is taken "sufficiently large".

In $I = [-5, 5]$ we consider the discontinuous functions

$$
f_1(x) = \begin{cases} e^{\frac{1}{x+5.5}}, & -5 \leq x < -3 \\ \cos(3x), & -3 \leq x < 2 \\ -\frac{x^3}{30} + 2, & 2 \leq x \leq 5. \end{cases} \qquad f_2(x) = \begin{cases} \log(-\sin(x/2)), & -5 \leq x < -2.5 \\ \tan(x/2), & -2.5 \leq x < 2 \\ \arctan(e^{-\frac{1}{x-5.1}}), & 2 \leq x \leq 5. \end{cases}
$$

We evaluate the constructed interpolants on a set of 5000 equispaced evaluation points $\Xi = \{\bar{x}_i = -5 + \frac{i}{1000} : i = 0, \dots, 5000\}$ and compute the Relative Maximum Absolute Error RMAE $= \max_i \frac{|r_n(\bar{x}_i) - f(\bar{x}_i)|}{|f(\bar{x}_i)|}$ and the same for r_n^S.

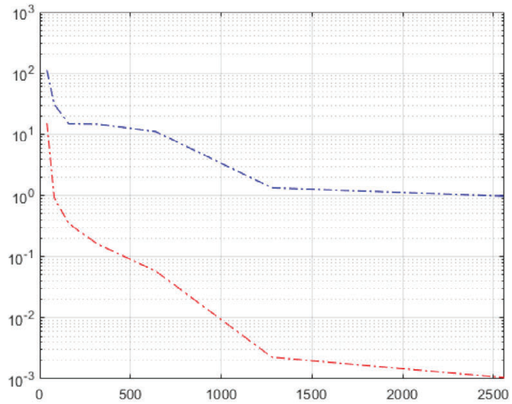

(a) Interpolation of f_1 with $d = 1$.

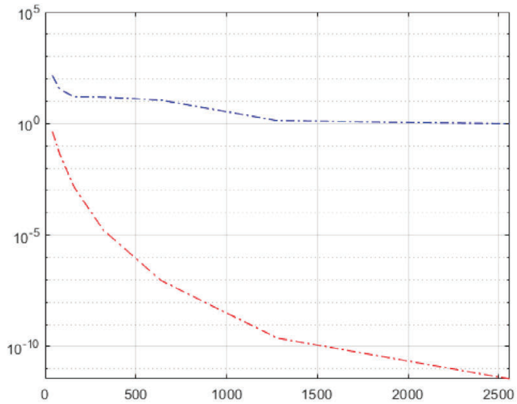

(b) Interpolation of f_1 with $d = 8$.

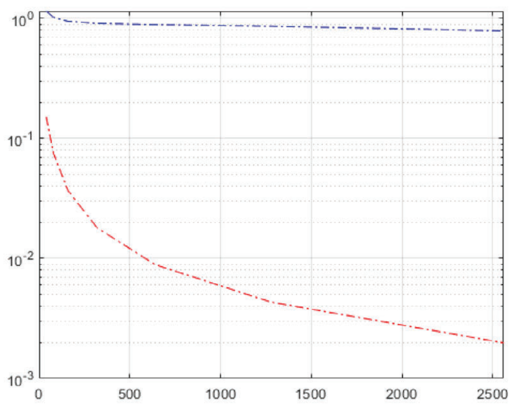

(c) Interpolation of f_2 with $d = 1$.

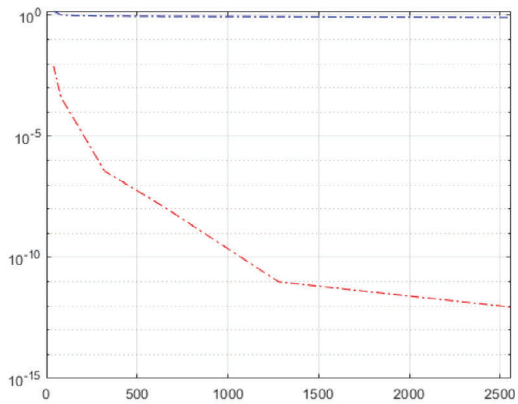

(d) Interpolation of f_2 with $d = 8$.

Fig. 1. The RMAE for f_1 and f_2 when one doubles the number of nodes from 40 to 2560. In blue, the standard interpolant $R_{n,d}$. In red, the proposed interpolant $R^s_{n,d}$. (For interpretation of the references to color in this figure legend, the reader is referred to the web version of this article.)

The FH interpolants

Here, we take various sets of equispaced nodes $\mathcal{X}_n = \{-5 + \frac{5i}{n} \,:\, i = 0, \ldots, n\}$, varying the size of n. The results are displayed in Fig. 1. We observe that the proposed reconstruction via the fake nodes approach by far outperforms the standard technique.

Fig. 2 displays a comparison between the direct application of the FH interpolant and the one modified by the SGA.

The AAA algorithm

As the starting set for the AAA algorithm, we consider 10 000 nodes randomly uniformly distributed in I, which we denote by $\mathcal{X}_{rand}$.

Looking at Table 1, we observe that using the AAA algorithm with starting set $S(\mathcal{X}_{rand})$ (indicated in the Table as AAA^S), that is, constructing the approximants via the fake nodes approach, does not suffer from the effects of the Gibbs phenomenon. For both approximants we fix the maximum degree to 20 and to 40 (by default 100 in the algorithm).

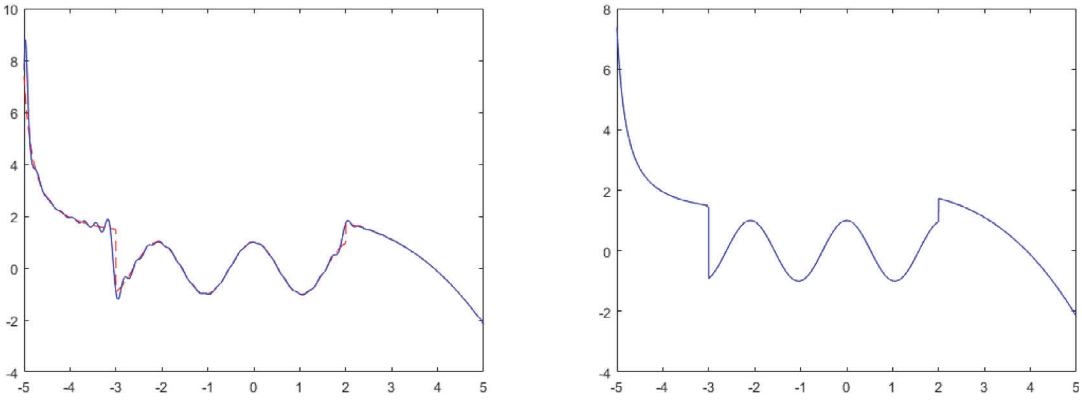

(a) Direct approximation. (b) Using the proposed approach.

Fig. 2. Interpolation of the function f_1 using 80 nodes and $d = 8$ in the FH interpolant. In red the function and in blue the interpolant. (For interpretation of the references to color in this figure legend, the reader is referred to the web version of this article.)

Table 1
RMAE for AAA and AAA^s approximants.

f	m_{max}	AAA	AAA^s
f_1	20	1.5674e+02	8.5189e−05
	40	1.4308e+00	2.9550e−09
f_2	20	3.6034e+02	2.2066e−07
	40	1.4656e+00	6.3485e−11

5. Conclusions

This work introduces an extension of the fake nodes approach to barycentric rational approximation, in particular to the family of FH interpolants and to the AAA algorithm for approximation, focusing on the treatment of the Gibbs phenomenon via the S-Gibbs algorithm. The results show that the proposed reconstructions outperform their classical versions, as they are not affected by distortions and oscillations.

CRediT authorship contribution statement

J.-P. Berrut: Supervision, Writing - review & editing. **S. De Marchi:** Supervision, Writing - review & editing, Funding acquisition. **G. Elefante:** Conceptualization, Methodology. **F. Marchetti:** Conceptualization, Methodology.

Acknowledgments

This work has been performed within the Italian Network on Approximation (RITA), and with the support of the GNCS-INdAM funds 2019 and NATIRESCO BIRD181249 project.

References

[1] M.S. Floater, K. Hormann, Barycentric rational interpolation with no poles and high rates of approximation, Numer. Math. 107 (2) (2007) 315–331.
[2] J.-P. Berrut, Rational functions for guaranteed and experimentally well-conditioned global interpolation, Comput. Math. Appl. 15 (1) (1988) 1–16.
[3] K. Hormann, Barycentric interpolation, in: Approximation Theory XIV: San Antonio 2013, in: Springer Proc. Math. Stat., vol. 83, Springer, Cham, 2014, pp. 197–218.

[4] A. Abdi, J.-P. Berrut, S.A. Hosseini, The linear barycentric rational method for a class of delay Volterra integro-differential equations, J. Sci. Comput. 75 (3) (2018) 1757–1775.
[5] W.-H. Luo, T.-Z. Huang, X.-M. Gu, Y. Liu, Barycentric rational collocation methods for a class of nonlinear parabolic partial differential equations, Appl. Math. Lett. 68 (2017) 13–19.
[6] S. De Marchi, K. Hormann, G. Klein, Barycentric rational interpolation at quasi-equidistant nodes, Dolomites Res. Notes Approx. 5 (Special Issue) (2012) 1–6.
[7] R. Baltensperger, Some results on linear rational trigonometric interpolation, Comput. Math. Appl. 43 (2002) 737–746.
[8] J.-P. Berrut, G. Elefante, A periodic map for linear barycentric rational trigonometric interpolation, Appl. Math. Comput. 371 (2020) 124924.
[9] R. Baltensperger, J.-P. Berrut, The linear rational collocation method, J. Comput. Appl. Math. 134 (1–2) (2001) 243–258.
[10] L. Bos, S. De Marchi, K. Hormann, J. Sidon, Bounding the Lebesgue constant for Berrut's rational interpolant at general nodes, J. Approx. Theory 169 (2013) 7–22.
[11] J.-P. Berrut, The conditioning of a linear barycentric rational interpolant, submitted for publication.
[12] Y. Nakatsukasa, O. Sète, L.N. Trefethen, The AAA algorithm for rational approximation, SIAM J. Sci. Comput. 40 (3) (2018) A1494–A1522.
[13] A. Gopal, L.N. Trefethen, Representation of conformal maps by rational functions, Numer. Math. 142 (2) (2019) 359–382.
[14] S.-I. Filip, Y. Nakatsukasa, L.N. Trefethen, B. Beckermann, Rational minimax approximation via adaptive barycentric representations, SIAM J. Sci. Comput. 40 (4) (2018) A2427–A2455.
[15] M.D. Buhmann, S. De Marchi, E. Perracchione, Analysis of a new class of rational RBF expansions, IMA J. Numer. Anal. (2019) http://dx.doi.org/10.1093/imanum/drz015.
[16] D. Gottlieb, C.-W. Shu, On the Gibbs phenomenon and its resolution, SIAM Rev. 39 (4) (1997) 644–668.
[17] S. De Marchi, W. Erb, F. Marchetti, Spectral filtering for the reduction of the Gibbs phenomenon for polynomial approximation methods on Lissajous curves with applications in MPI, Dolomites Res. Notes Approx. 10 (2017) 128–137, Special Issue.
[18] S. De Marchi, F. Marchetti, E. Perracchione, D. Poggiali, Polynomial interpolation via mapped bases without resampling, J. Comput. Appl. Math. 364 (2020) 112347, 12.
[19] J.-P. Berrut, L.N. Trefethen, Barycentric Lagrange interpolation, SIAM Rev. 46 (3) (2004) 501–517.
[20] N.J. Higham, The numerical stability of barycentric Lagrange interpolation, IMA J. Numer. Anal. 24 (4) (2004) 547–556.